SANDIA REPORT
SAND2000-0339
Unlimited Release
Printed February 2000

Thermal Spray and Cold Spray Analysis of Density, Porosity, and Tensile Specimens for Use with LIGA Applications

M. K. Decker and M. F. Smith

Prepared by
Sandia National Laboratories
Albuquerque, New Mexico 87185 and Livermore, California 94550

Sandia is a multiprogram laboratory operated by Sandia Corporation, a Lockheed Martin Company, for the United States Department of Energy under Contract DE-AC04-94AL85000.

Sandia National Laboratories

Issued by Sandia National Laboratories, operated for the United States Department of Energy by Sandia Corporation.

Available to DOE and DOE contractors from
Office of Scientific and Technical Information
P.O. Box 62
Oak Ridge, TN 37831

Prices available from (703) 605-6000
Web site: http://www.ntis.gov/ordering.htm

Available to the public from
National Technical Information Service
U.S. Department of Commerce
5285 Port Royal Rd
Springfield, VA 22161

DISCLAIMER

Portions of this document may be illegible in electronic image products. Images are produced from the best available original document.

SAND2000-0339
Unlimited Release
Printed February 2000

Thermal Spray and Cold Spray Analysis of Density, Porosity, and Tensile Specimens for Use with LIGA Applications

M.K. Decker
Advanced Weapon Technologies

M.F. Smith
Joining, Coating & Net Shaping

Sandia National Laboratories
P.O. Box 5800
Albuquerque, NM 87185-0481

Abstract

This analysis provides a preliminary investigation into using Twin-Wire Arc Thermal Spray and Cold Spray as material deposition processes for LIGA applications. These spray material processes were studied to make an initial determination of their potential as alternatives to producing mechanical parts via the electroplating process. Three materials, UltraMachinable® Stainless Steel, BondArc®, and aluminum, were sprayed using Thermal Spray. Only aluminum was sprayed using the Cold Spray process. Following the spray procedure, the test specimens were released from a copper mold and then tested. Three tests, density, tensile strength, and porosity, were performed on the specimens to determine the spray effect on material properties. Twin-Wire Arc Thermal Spray did not demonstrate adequate deposition properties and does not appear to be a good process candidate for LIGA. However, Cold Spray yielded better density results and warrants further investigation to analyze the minimum feature size produced by the process.

Key Words

Cold Spray, Electroplating, Thermal Spray, Twin-Wire Arc Thermal Spray, Flame Spray, LIGA, Mechanical Properties, Coating, Mechanical Properties of Coatings.

Acknowledgements

The authors wish to thank the following laboratory personnel for their efforts: R.O. Cote (Department 1831) was the operator for the Twin-Wire Arc Thermal Spray deposition process; D.L. Gilmore and T.J. Roemer (Department 1831) were the two operators for the Cold Spray deposition process; D.T. Schmale (Department 1831) tested UltraMachinable® Stainless Steel tensile specimens, BondArc® tensile specimens, Twin-Wire Arc Thermal Spray aluminum tensile specimens, and all Cold Spray aluminum tensile specimens; A.C. Kilgo (Department 1822) performed area-fraction of void measurements on UltraMachinable® Stainless Steel specimens, BondArc® specimens, and aluminum specimens; and J. Baum, Tech Reps, Inc., provided technical editing and documentation preparation support.

Contents

Figures

Tables

1.0 Introduction

This investigation provides a preliminary analysis of the potential applicability of spray materials as a manufacturing process to fabricate LIGA hardware from alternative metals that cannot be deposited by the electroplating process. The LIGA fabrication process is an additive process in which material is deposited, typically by electroplating, into a precision mold of PMMA (polymethyl methacrylate) realized through deep X-ray lithography. (LIGA is an acronym derived from the German words for lithography, electroplating, and molding—Lithographie, Galvanoformung, and Abformung.)

Currently, the only materials that can be readily deposited using the electroplating process are copper, nickel, permalloy (80% Ni and 20% Fe), and gold. Developing alternatives to electroplating would allow designers the choice of using other materials, including ceramics or nonmetals, when designing mechanical parts or structures.

This study tested Twin-Wire Arc Thermal Spray and Cold Spray to determine the potential applicability of metal spray deposition processes as alternatives to electroplating. If spraying materials could provide such an option, the time required for the deposition process would be decreased to minutes instead of hours, which is the current timeframe needed for the electroplating process. Such an alternative would in turn decrease the costs associated with depositing materials. Also, the spraying processes would be safer for the environment than typical electroplating operations. The initial investigation attempted to determine whether spray materials are a potential alternative to electroplating. If so, future studies will determine whether such spraying materials, when combined with alternative metals, could effectively produce quality mechanical parts that would be durable enough to be practical and cost-effective.

In the Twin-Wire Arc Thermal Spray deposition process, two wires of the metal to be spray deposited are brought together at an angle, and an electric arc is struck between the wire tips. The heat of the arc causes the metal at the wire tips to become continuously melted, which makes the wires consumable electrodes. As the metal is melted at the wire tips, a jet of compressed air, in a specially shaped aircap surrounding the wire tips, is used to strip the molten metal from the wire tips and atomize it into small droplets. The air jet then propels the small droplets onto the target surface, in this case, the LIGA mold surface. As the droplets strike the surface, they flow out and solidify at very high rates, typically 10^6 to 10^8 K/sec. In general, one droplet completely solidifies before the next droplet impacts the same location.

In the Cold Spray Process [1], a supersonic jet of compressed gas is used to accelerate near-room-temperature powder particles, typically 10 to 50 microns in diameter, up to velocities in the range of 500 to 1500 m/s. Under proper conditions, when the solid powder particles impact a solid surface, their kinetic energy is sufficient to cause plastic deformation and consolidation of the arriving particles with the underlying material (by a process thought to be analogous to explosive welding [2]). Because Cold Spray is a near-room-temperature, solid-state process, potential advantages of its use include eliminating cool-down induced stresses in the finished part and the possibility of avoiding undesirable phases, oxidation, and grain growth during the deposition process.

2.0 Design of Molds

Molds were used in the investigation to create reverse images, or pockets, for each fabricated part. The molds were filled with sprayed materials to fabricate the desired part.

For several reasons, copper was the metal chosen for the molds. Copper is able to withstand the heat input of the deposited materials, aluminum, nickel, and stainless steel, which were sprayed into the molds. Also, each mold had to be made of a material that could be electroplated using the LIGA process. Additionally, once the sprayed materials were deposited, the mold had to be etched away to release the sprayed materials in the mold. Copper met these requirements due to its compatibility with the LIGA fabrication process and its ability to be easily etched with a wide variety of chemical etch solutions without effecting the deposited material.

The copper molds were machined conventionally. Eight slots, shown in Figure 1, were used for obtaining bulk density and porosity data. A tensile specimen was placed in the center of the mold and was used to determine modulus and ultimate tensile strength, as shown in Figure 2. A photograph of the mold is shown in Figure 3.

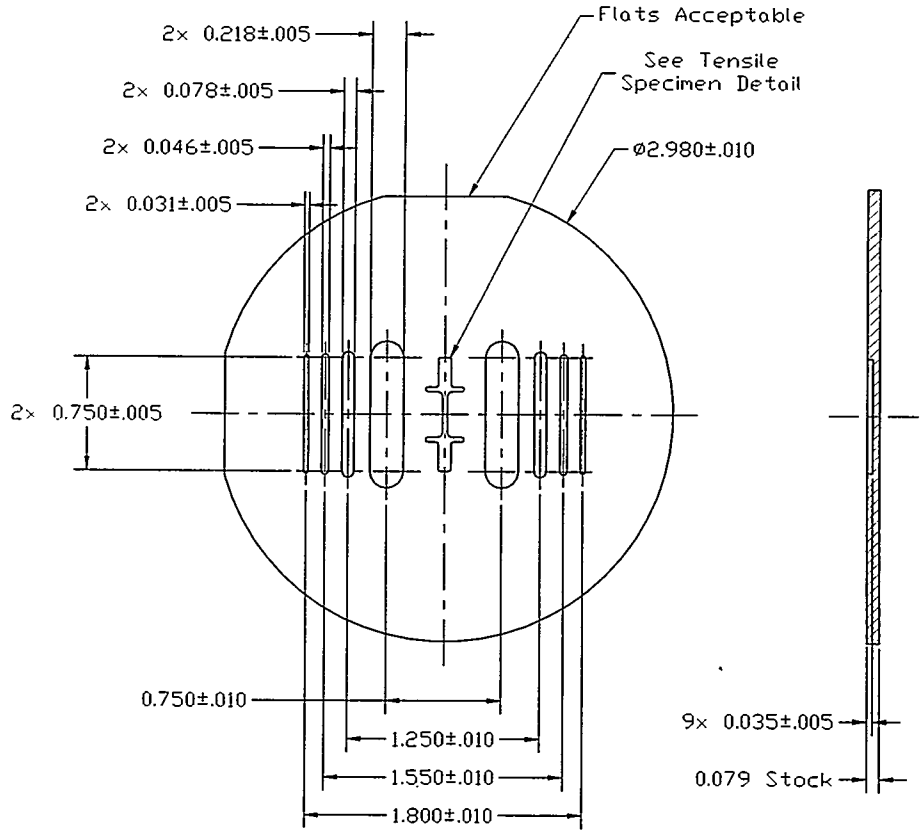

Figure 1. Conventionally Machined Copper Structure.

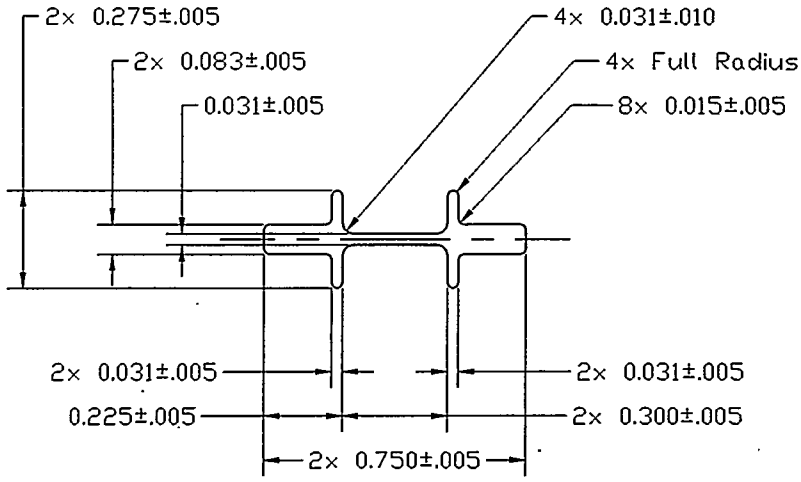

Figure 2. Detail of Tensile Specimen.

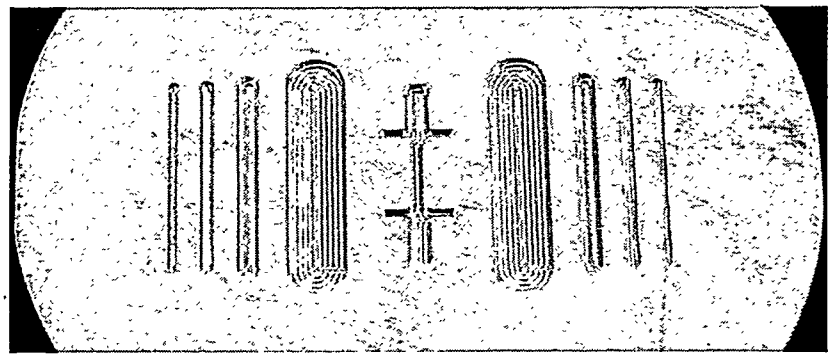

Figure 3. Photograph of Copper Mold.

3.0 Spray Materials Used

Before spraying any material into the molds, each mold was cleaned to eliminate possible unknown reactions between the mold and the sprayed material. The copper mold was cleaned in a 5% H_2SO_4 (sulfuric acid) solution to remove any contaminates or oxide from the surface of the copper mold. For each mold, the elapsed time between cleaning the copper mold and spraying the thermal or Cold Spray material was approximately 5 minutes. Because copper oxidizes at a rate of 0.5 microns per year in a typical ambient environment [3], the amount of copper oxidized between the time of cleaning and material deposition was estimated to be 5 picometers. This amount of oxidation was considered negligible because the test equipment used was not sensitive to measurements of this magnitude.

3.1 Twin-Wire Arc Thermal Spray

A Hobart/Tafa Model 9000 Twin-Wire Arc Spray System was used to spray deposit the following three test metals. The first metal tested was the Hobart/Tafa 88T UltraMachinable® Stainless Wire, which is a specially formulated 300 Series Stainless Steel. The second metal tested was Hobart/Tafa Arc Spray BondArc® Wire – 75B™, which is composed of 95% nickel and 5% aluminum. The third metal tested was Hobart/Tafa Arc Spray Aluminum Wire – 01T, which is composed of at least 99.5% aluminum. The values are all weight percent.

During the Twin-Wire Arc Thermal Spray deposition process, each mold was attached to a spindle, which was then rotated at an angular velocity of approximately 150 rpm. The Twin-Wire Arc machine settings, recommended by the manufacturer, for spraying UltraMachinable® Stainless (88T), BondArc® (75B), and aluminum (01T) are described in Table 1.

Table 1. Thermal Spray Machine Parameters.

	88T	75B	01T
Supply (psi)	80	80	80
Main (psi)	60	60	60
Arc Jet (psi)	60	60	60
Amps	55	75	50 - 75
Volts	32	32	29 – 30
Standoff (inches)	5 – 7	5 – 7	3 – 4
Head Configuration	Blue Cap, Short Cross	Green Cap, Long Cross	Green Cap, Long Cross

3.2 Cold Spray

For this evaluation, only one Cold Spray material, a 99.8% pure aluminum powder, was spray deposited into a copper mold. The nominal size of the aluminum powder was 20 microns in diameter, the particle velocity was approximately 850 m/s with a gas supply pressure of 200-300 psi, and the temperature of the compressed helium gas was 100°C. Two separate sprays were performed, with one spray done in the direction of the mold features, and the other spray against the direction of the features in the mold. For the relatively large size of the specimens, no significant differences were noticed during the analysis of the specimens. Therefore, no distinctions were made between the direction of the spray into the LIGA molds.

4.0 Post Spray Machining

After each mold was sprayed, a grinding process was performed to remove excess material spray deposited above the mold surface during the spray procedure. After the molds were ground, excess copper was removed from the outer edges of the mold, reducing the size of the mold to one inch wide by two inches long. By removing the excess copper from the mold, multiple molds could be lapped simultaneously, and less copper had to be removed during the etching process. Finally, 15-micron diamond slurry was used to lap the tensile specimen in the

mold. This lapping process removed many of the large scratches in the tensile specimen caused by the grinding process, as well as polishing the tensile specimens to a uniform thickness. The pre-grinding condition of the mold is displayed in the top photograph in Figure 4. The post-lapping condition of the mold is displayed in the bottom photograph in Figure 4.

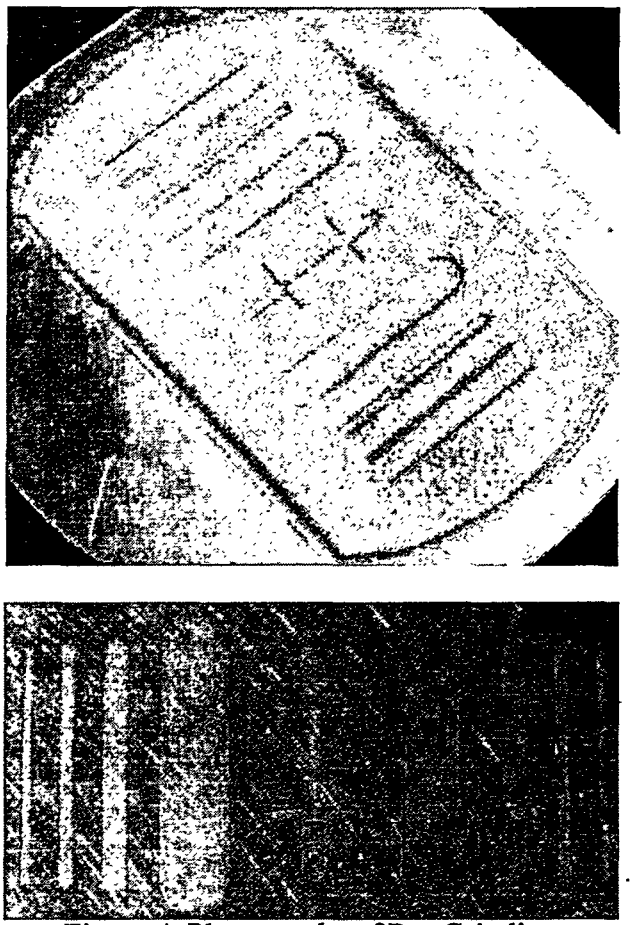

Figure 4. Photographs of Pre-Grinding and Post-Lapping Machining.

5.0 Etching of Copper

A chemical etch system manufactured by Enthone-OMI was chosen to release the density, porosity, and tensile specimens from the copper molds. Enstrip® C-38 was used because of its ability to etch copper, while not etching the specimens in the copper molds. Enstrip® C-38 is a two-part system composed of Part A and Part B. The active ingredients in Part A are ammonium hydroxide and ammonium salts. The active ingredient in Part B is sodium chloride. The solution concentration consisted of 600 ml of Part A 200 ml of Part B. With this quantity of Enstrip® C-38, three molds could be etched in approximately 15 hours at room temperature. Completing the etching process required approximately three hours on the first mold, five hours on the second and seven hours on the third mold. After etching the copper from the three molds, no appreciable amount of additional copper could be consumed.

6.0 Experiment Results

6.1 Twin-Wire Arc Thermal Spray UltraMachinable® Stainless Steel

6.1.1 Density

Density data were obtained from the various specimens of different width within each mold by measuring their physical dimensions and weighing them to obtain their mass. From this data, an average density was calculated. An uncertainty analysis was performed on the measurements taken to calculate the density data. The method of the uncertainty analysis is described in Section 6.1.2. The normalized density was computed by dividing the average density by the theoretical density. Mold aspect ratio was computed by dividing the mold depth by the mold width. The data are listed below in Table 2. The theoretical density of Twin-Wire-Arc Thermal Spray UltraMachinable® Stainless Steel is 6.93 g/cc [4]. Figure 5 shows a graph of normalized density vs. mold aspect ratio.

Two molds were sprayed with UltraMachinable® Stainless Steel. Four of the specimens from one mold were set aside for porosity measurements. One of the specimens from this group (with mold aspect ratio of 0.16) did not have a proper fill and was not used for these calculations.

Table 2. Physical Properties of Thermal Spray UltraMachinable® Stainless Steel.

Dimensions (cm)			Volume	Mass	Density	Uncertainty	Normalized	Mold
Length	Width	Thickness	(cc)	(g)	(g/cc)	(g/cc)	Density	Aspect Ratio
2.456	0.559	0.079	0.103	0.550	5.350	0.014	0.77	0.16
2.452	0.558	0.079	0.102	0.583	5.693	0.015	0.82	0.16
2.099	0.206	0.077	0.033	0.180	5.495	0.031	0.79	0.45
2.101	0.203	0.076	0.032	0.180	5.652	0.032	0.82	0.45
2.101	0.202	0.076	0.032	0.184	5.813	0.032	0.84	0.45
2.014	0.126	0.079	0.020	0.104	5.286	0.051	0.76	0.76
2.012	0.121	0.076	0.018	0.105	5.751	0.055	0.83	0.76
2.012	0.119	0.081	0.019	0.105	5.449	0.052	0.79	0.76
1.976	0.081	0.081	0.013	0.055	4.250	0.077	0.61	1.13
1.977	0.081	0.080	0.013	0.055	4.315	0.078	0.62	1.13
1.972	0.080	0.080	0.013	0.060	4.794	0.080	0.69	1.13

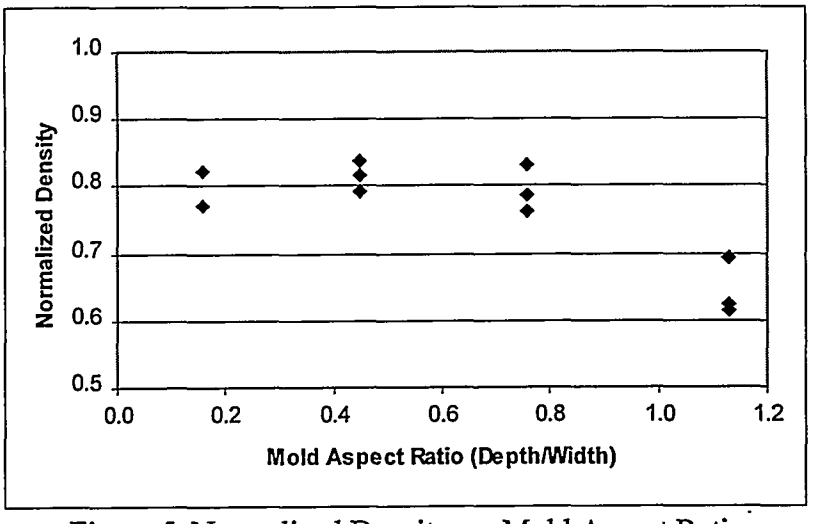

Figure 5. Normalized Density vs. Mold Aspect Ratio for Theramal Spray UltraMachinable® Stainless Steel.

6.1.2 *Uncertainty Analysis for Density*

The uncertainty in the density measurement for each specimen arises from the measurement error incurred by reading the physical sizes of the specimen as well as the mass of the specimen. (Density is given by $\rho = m/V$.) Uncertainty is quantified by determining the sensitivity of the data to the physical measurements, multiplying by the expected error, and then combining the results as root squares [5]. Symbolically, this is given by the following equation:

$$\Delta\rho = \sqrt{\left(\frac{\partial\rho}{\partial m}\Delta m\right)^2 + \left(\frac{\partial\rho}{\partial V}\Delta V\right)^2}$$

where $\Delta\rho$ is the total uncertainty of the density measurement, ρ is the density, m is the mass, and V is the volume of the specimen. By taking partial derivatives of density with respect to mass and volume, the results are given by the following equations:

$$\frac{\partial\rho}{\partial m} = \frac{1}{V} \qquad \frac{\partial\rho}{\partial V} = -\frac{m}{V^2}$$

The above equations can then be reduced to the following:

$$\frac{\Delta\rho}{\rho} = \sqrt{\left(\frac{\Delta m}{m}\right)^2 + \left(\frac{\Delta V}{V}\right)^2}$$

The expected error of the mass measurements, Δm, is 0.001 g because of the resolution of the mass balance. The volume of the specimens is given by the following equation:

$$V = (l - w)wt + \frac{\pi w^2}{4}t$$

where l is the length, w is the width, and t is the thickness of the specimen. The expected error of the volume calculations is given by the following equations:

$$\Delta V = \frac{\partial V}{\partial l}\Delta l + \frac{\partial V}{\partial w}\Delta w + \frac{\partial V}{\partial t}\Delta t$$

$$\Delta V = (wt)\Delta l + t(l - 2w + \frac{\pi w}{2})\Delta w + w(l - w + \frac{\pi w}{4})\Delta t$$

The expected error of the size measurements, Δl, Δw, and Δt, are 0.0013 cm because of the resolution of the caliper used.

6.1.3 Tensile

To conduct a tensile test, the specimen is first placed in a mounting jig and inserted into a load cell. The load cell is then zeroed, and the screws of the mounting jig are tightened [6]. Next a laser beam was centered on the tabs of the specimen to measure the strain. The strain rate at which the specimens were tested was 0.001 sec^{-1}. Figure 6 shows two specimens that were tested.

It is noteworthy that the modulus listed in Table 3 for the sprayed material is much lower than that of wrought material of a similar composition. This is commonly observed in spray-deposited materials. The true modulus of elasticity, or Young's modulus, is the ratio of the stress, σ, to the reversible strain, ε, and is related to elastic stretching of interatomic bonds. It is a fundamental property of the material that should be independent of microstructure or processing. The fact that the observed slopes of the stress/strain plots differ significantly from published values for similar material implies that the stress/strain ratio in this region is not truly representative of Young's modulus. Although the plots appear to be nearly linear, it is likely that there is some non-elastic strain in this region, most likely due to microcracking between the solidified spray particles. If the rate of microcracking were essentially constant over this range, the plot would still appear essentially linear; however, if the stress were removed, the non-elastic (microcracking) portion of the strain would not be recovered. With this in mind, in this paper we will refer to the slope of the stress/strain plots in the nearly linear region as a "pseudo" modulus of elasticity.

Table 3 shows the "pseudo" modulus of elasticity and fracture stress for UltraMachinable® Stainless Steel. A reference for AISI 303 stainless steel is listed [7]. Coatings typically have a lower modulus in tension because of the microcracking at the splat boundaries. Note: Because the 2% offset yield strength is unavailable for the UltraMachinable® Stainless Steel tensile specimens, fracture strength of the specimens is compared to the tension strength of AISI 303 stainless steel.

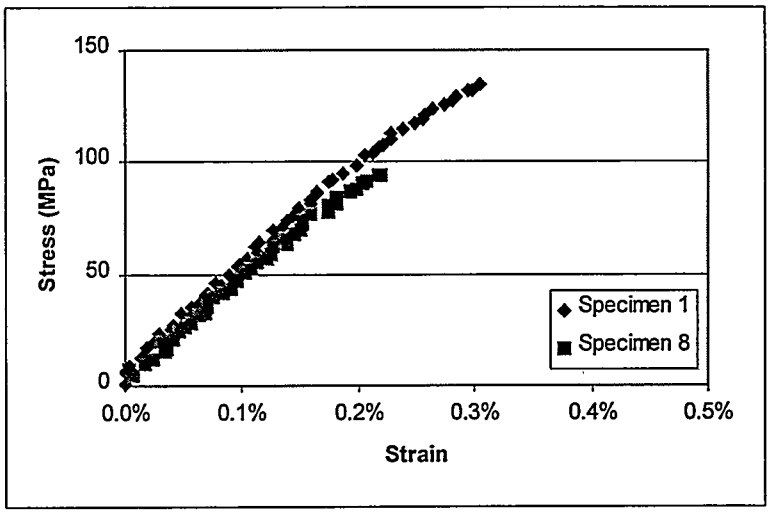

Figure 6. Engineering Stress vs. Engineering Strain for Thermal Spray UltraMachinable® Stainless Steel.

Table 3. Modulus and Yield Strength for Thermal Spray UltraMachinable® Stainless Steel.

	Modulus (GPa)	Fracture Strength (MPa)
Specimen 1	48	134
Specimen 8	46	94
AISI 303 Stainless Steel	193	585

6.1.4 Porosity

Gray-scale images were taken using a Reichert Metallograph in "brightfield" mode. Each image was taken in a fairly random location to prevent skewing of the data. The only exception to this was when the magnification was chosen to prevent inclusion of the surrounding copper. A duplicate gray-scale image was made for analysis, with the original image being used for comparison. Using a histogram, the image was "thresholded" to show the voids as black and the rest of the material as light. Each image was "thresholded" in the same manner, and the reading of the area-fraction of voids was then recorded. The image analysis software used was PGT Imagist 2 PC. Volume-fraction of voids, or porosity, was equal to the area-fraction of voids in the unbiased analysis [8]. Figure 7 shows the porosity vs. mold aspect ratio for UltraMachinable® Stainless Steel. Table 4 shows the average porosity, standard deviation, and percent accuracy for the material.

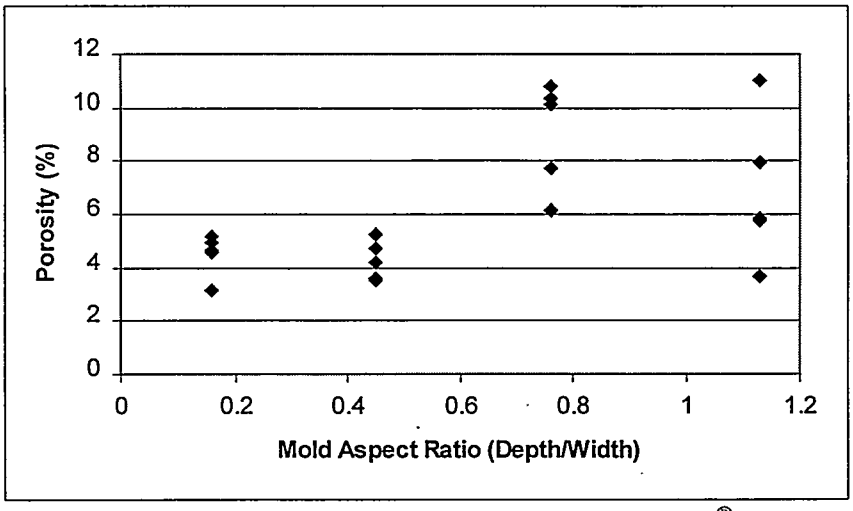

Figure 7. Porosity vs. Mold Aspect Ratio for UltraMachinable® Stainless Steel.

Table 4. Porosity Data for UltraMachinable® Stainless Steel.

Mold Aspect Ratio	Number of Measurements	Average % Porosity	Standard Deviation	% Accuracy
0.16	5	4.50	0.79	15.63
0.45	5	4.26	0.73	15.37
0.76	5	9.02	2.02	19.99
1.13	5	6.88	2.78	36.17

6.1.5 Determination of Percent Accuracy for Porosity

The level of precision, or percent accuracy, can be calculated with a 95% confidence level from the following equation, if estimates of the mean, standard deviation, and sample size are known.

$$\%\ Accuracy = \frac{200\,\sigma(P)}{\sqrt{N}\,\mu(P)}$$

where $\sigma(P)$ is the standard deviation, $\mu(P)$ is the mean, and N is the number of samples obtained for the porosity measurements [8,9].

6.1.6 *Conclusions for Thermal Spray UltraMachinable® Stainless Steel*

An analysis of variance was used to test multiple data samples to determine whether the specimens were taken from the same population, and thus would be considered measurements of the same sample data. Figure 8 shows the results of this analysis for UltraMachinable® Stainless Steel.

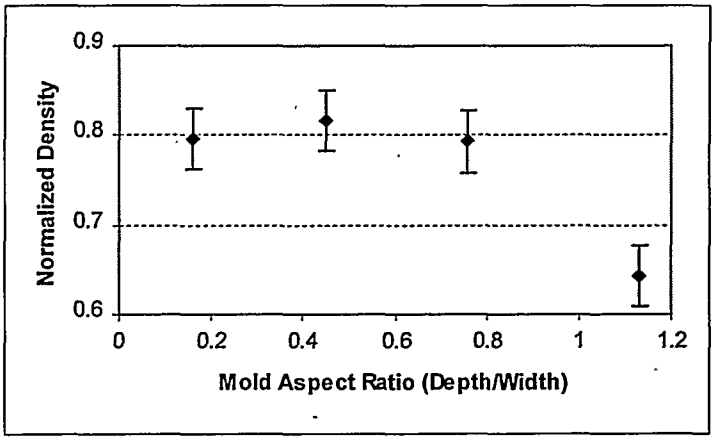

Figure 8. Mean Normalized Density vs. Mold Aspect Ratio for Thermal Spray UltraMachinable® Stainless Steel.

Based on the analysis of variance of the density measurements, up to an aspect ratio of 0.8, it was observed that the normalized density stays fairly uniform. At higher aspect ratios, the normalized density decreases dramatically from 0.8 to 0.65. This change indicates that some higher order effects may be occurring at this higher aspect ratio. An increase in porosity at higher aspect ratios can also be seen in the porosity data. The porosity of the specimens is likely to be lower than one minus the normalized density, due to polishing effects on the specimens. As a specimen is polished, material can be deposited into the pores, or metal smeared to close a small pore, causing a lower porosity reading. At an aspect ratio greater than 0.5, the porosity increases from 4% to 9%. This change also indicates that another process may be occurring at these higher aspect ratios. Correlation analysis compares two sets of data to determine whether their curves have the same shape. A correlation coefficient near or equal to zero implies little or no relationship. In contrast, if a value is closer to 1 or –1, then there is a stronger relationship between the two variables. A positive correlation indicates a direct relationship between the two variables; a negative correlation indicates an inverse relationship between the two variables. Table 5 shows the correlation coefficients between mold aspect ratio, average density, and average porosity for UltraMachinable® Stainless Steel.

Table 5. Correlation Coefficients for Thermal Spray UltraMachinable® Stainless Steel.

Stainless Steel	Correlation
Aspect Ratio and Density	-0.815
Aspect Ratio and Porosity	0.662
Density and Porosity	-0.291

Although the correlation coefficient is relatively high for the aspect ratio and the density, it does not meet the 0.9 criteria for this analysis and, therefore, will not be used as an indicator to predict one variable from the other. The tensile specimens were brittle, making it difficult to obtain accurate yield strength comparisons, but a "pseudo" modulus of elasticity was obtained and proved to be 25% of the AISI 303 stainless steel modulus. Because its normalized density is lower than 0.9 and porosity is not a good predictor of density, Twin-Wire Arc Thermal Spray UltraMachinable® Stainless Steel does not appear to be a good candidate for further study.

6.2 Twin-Wire Arc Thermal Spray BondArc®

6.2.1 Density

The density data for Thermal Spray BondArc® are listed in Table 6. The theoretical density of Thermal Spray BondArc® is 7.8 g/cc [10]. Figure 9 shows a graph of normalized density vs. mold aspect ratio.

Table 6. Physical Properties of Thermal Spray BondArc®.

Dimensions (cm)			Volume	Mass	Density	Uncertainty	Normalized	Mold
Length	Width	Thickness	(cc)	(g)	(g/cc)	(g/cc)	Density	Aspect Ratio
2.454	0.559	0.084	0.109	0.709	6.486	0.016	0.83	0.16
2.459	0.559	0.080	0.105	0.690	6.599	0.016	0.85	0.16
2.456	0.559	0.084	0.109	0.710	6.488	0.016	0.83	0.16
2.454	0.556	0.080	0.104	0.693	6.671	0.016	0.86	0.16
2.449	0.554	0.081	0.105	0.683	6.514	0.016	0.84	0.16
2.101	0.206	0.076	0.032	0.206	6.390	0.031	0.82	0.45
2.101	0.202	0.079	0.033	0.210	6.420	0.031	0.82	0.45
2.103	0.201	0.083	0.034	0.219	6.418	0.030	0.82	0.45
2.101	0.201	0.084	0.035	0.210	6.068	0.029	0.78	0.45
2.098	0.201	0.076	0.031	0.204	6.492	0.032	0.83	0.45
2.009	0.119	0.079	0.019	0.120	6.436	0.054	0.83	0.76
2.009	0.119	0.083	0.020	0.120	6.139	0.051	0.79	0.76
2.012	0.119	0.076	0.018	0.113	6.255	0.055	0.80	0.76
2.014	0.119	0.074	0.017	0.112	6.405	0.057	0.82	0.76
2.019	0.118	0.083	0.019	0.121	6.224	0.052	0.80	0.76
1.981	0.081	0.081	0.013	0.078	6.012	0.077	0.77	1.13
1.981	0.080	0.079	0.012	0.075	6.061	0.081	0.78	1.13
1.981	0.080	0.081	0.013	0.075	5.872	0.078	0.75	1.13
1.976	0.080	0.074	0.012	0.070	6.063	0.087	0.78	1.13
1.981	0.079	0.070	0.011	0.070	6.479	0.093	0.83	1.13

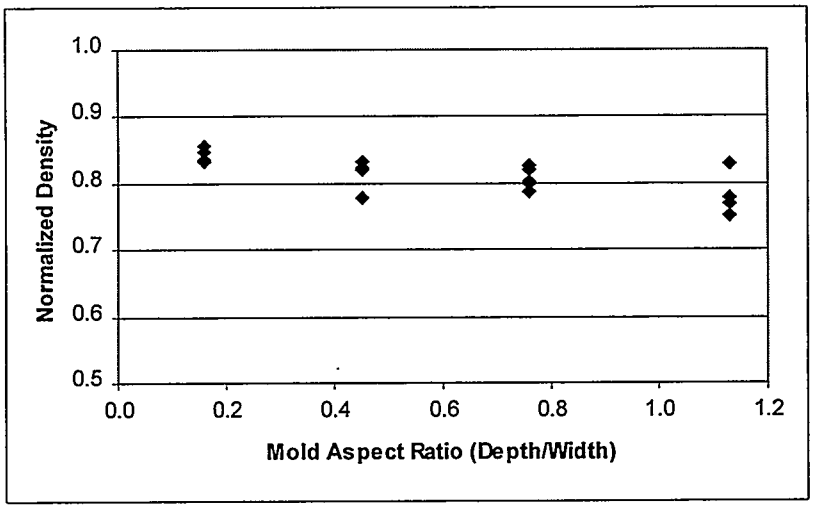

Figure 9. Normalized Density vs. Mold Aspect Ratio for Thermal Spray BondArc®.

6.2.2 *Tensile*

Figure 10 shows the three tensile specimens that were tested. Table 7 shows the modulus of elasticity and fracture stress for Thermal Spray BondArc®. A reference for pure nickel is also listed [11]. Coatings typically have a lower modulus in tension due to the microcracking at the splat boundaries. Note: Because the 2% offset yield strength is unavailable for the BondArc®, fracture strength of the Thermal Spray tensile specimens is compared to the tension strength of pure nickel.

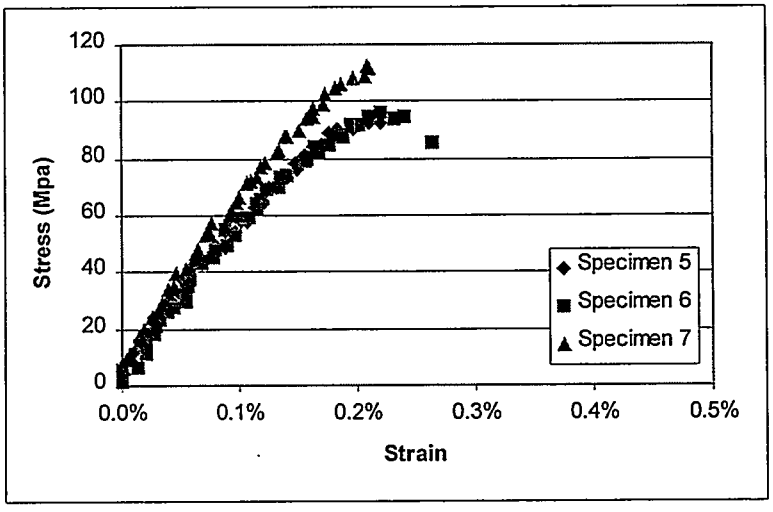

Figure 10. Engineering Stress vs. Engineering Strain for Thermal Spray BondArc®.

Table 7. Modulus and Yield Strength
for Thermal Spray BondArc®.

	Modulus (GPa)	Fracture Strength (MPa)
Specimen 5	47	93
Specimen 6	49	85
Specimen 7	56	112
Nickel	160	344

6.2.3 Porosity

Figure 11 shows the porosity vs. mold aspect ratio for Thermal Spray BondArc®. Table 8 shows the average porosity, standard deviation, and percent accuracy for Thermal Spray BondArc®.

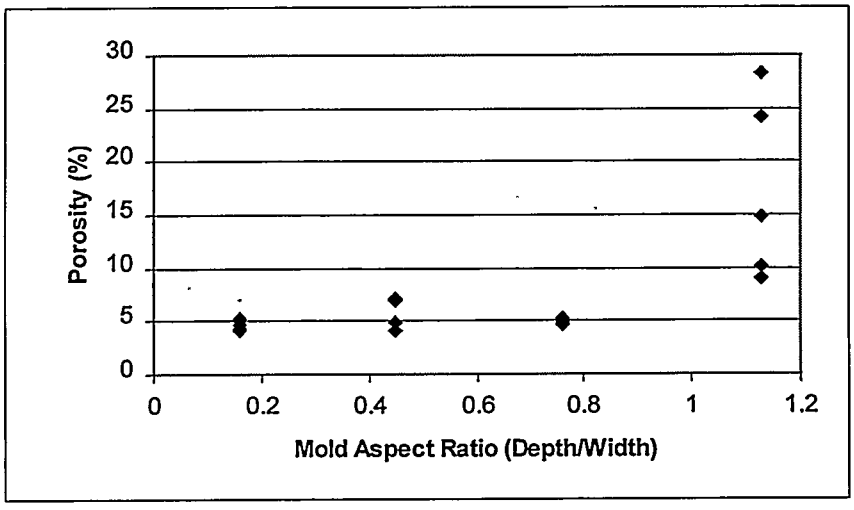

Figure 11. Porosity vs. Mold Aspect Ratio
for Thermal Spray BondArc®.

Table 8. Porosity Data for Thermal Spray BondArc®.

Mold Aspect Ratio	Number of Measurements	Average % Porosity	Standard Deviation	% Accuracy
0.16	5	4.72	0.45	8.47
0.45	5	6.06	1.46	21.51
0.76	5	4.93	0.24	4.36
1.13	5	17.28	8.61	44.55

6.2.4 *Conclusions for Thermal Spray BondArc®*

An analysis of variance was used to test multiple data samples to determine whether the specimens were taken from the same population, and thus would be considered measurements of the same sample data. Figure 12 shows the results of this analysis for Thermal Spray BondArc®.

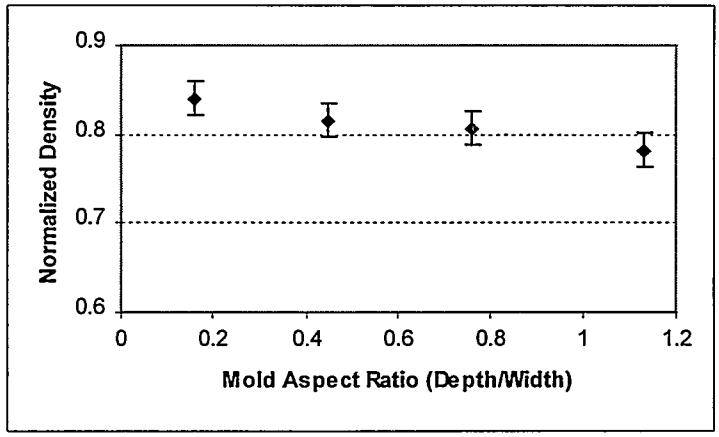

Figure 12. Mean Normalized Density vs. Mold Aspect Ratio for Thermal Spray BondArc®.

Based on the analysis of variance of the density measurements, it was observed that the normalized density consistently dropped as the aspect ratio increased. The porosity of the specimens is likely to be lower than one minus the normalized density, because of the polishing of the specimens. As a specimen is being polished, material can be deposited into the pores, or metal smeared to close a small pore, causing a lower porosity reading. An increase in porosity at higher aspect ratios can also be seen in the porosity data. At an aspect ration greater than 0.8, the porosity increases from 5% to 17%. Table 9 shows the correlation coefficients between mold aspect ratio, average density, and average porosity for Thermal Spray BondArc®.

Table 9. Correlation Coefficients for Thermal Spray BondArc®.

BondArc®	Correlation
Aspect Ratio and Density	-0.984
Aspect Ratio and Porosity	0.812
Density and Porosity	-0.829

The correlation coefficients are all relatively high, but the correlation coefficient for density and porosity does not meet the 0.9 criteria and, therefore, will not be used as an indicator to predict one variable from the other. The tensile specimens were brittle, making it difficult to obtain accurate yield strength comparisons, but a "pseudo" modulus of elasticity was obtained

and proved to be 31% of pure nickel. Because pure nickel can be plated in the LIGA process, Twin-Wire Arc Thermal Spray BondArc® will not be investigated further.

6.3 Twin-Wire Arc Thermal Spray and Cold Spray Aluminum

6.3.1 Density

The density data for Twin-Wire Arc Thermal Spray Aluminum is listed in Table 10. The theoretical density of aluminum is 2.7 g/cc [7,12]. The density data for Cold Spray Aluminum are listed below in Table 11. Figure 13 shows a graph of normalized density vs. mold aspect ratio for both Twin-Wire Arc Thermal Spray and Cold Spray Aluminum.

Table 10. Physical Properties of Twin-Wire Arc Thermal Spray Aluminum.

Dimensions (cm)			Volume	Mass	Density	Uncertainty	Normalized	Mold
Length	Width	Thickness	(cc)	(g)	(g/cc)	(g/cc)	Density	Aspect Ratio
2.459	0.556	0.065	0.084	0.177	2.100	0.013	0.78	0.16
2.438	0.554	0.053	0.069	0.140	2.044	0.015	0.76	0.16
2.446	0.554	0.080	0.103	0.180	1.746	0.010	0.65	0.16
2.438	0.554	0.076	0.098	0.190	1.941	0.011	0.72	0.16
2.443	0.551	0.062	0.080	0.167	2.094	0.013	0.78	0.16
2.452	0.544	0.053	0.068	0.140	2.067	0.015	0.77	0.16
2.421	0.541	0.053	0.067	0.146	2.195	0.016	0.81	0.16
2.098	0.206	0.053	0.023	0.040	1.775	0.044	0.66	0.45
2.090	0.206	0.076	0.032	0.060	1.870	0.031	0.69	0.45
2.101	0.203	0.053	0.022	0.040	1.794	0.045	0.66	0.45
2.102	0.203	0.066	0.028	0.056	2.027	0.036	0.75	0.45
2.101	0.203	0.061	0.025	0.054	2.119	0.039	0.78	0.45
2.098	0.203	0.079	0.033	0.060	1.825	0.030	0.68	0.45
2.083	0.196	0.056	0.022	0.043	1.928	0.045	0.71	0.45
2.012	0.122	0.064	0.015	0.030	1.952	0.065	0.72	0.76
2.015	0.121	0.074	0.018	0.030	1.697	0.057	0.63	0.76
2.014	0.119	0.053	0.013	0.025	1.974	0.079	0.73	0.76
2.012	0.119	0.053	0.013	0.025	1.977	0.079	0.73	0.76
2.015	0.119	0.067	0.016	0.030	1.876	0.063	0.69	0.76
2.019	0.119	0.079	0.019	0.030	1.601	0.053	0.59	0.76
2.008	0.111	0.053	0.012	0.024	2.043	0.085	0.76	0.76
1.969	0.088	0.054	0.009	0.016	1.724	0.108	0.64	1.13
1.976	0.084	0.053	0.009	0.017	1.942	0.114	0.72	1.13
1.979	0.081	0.053	0.009	0.017	1.999	0.118	0.74	1.13
1.980	0.081	0.065	0.010	0.020	1.936	0.097	0.72	1.13
1.980	0.081	0.066	0.011	0.020	1.899	0.095	0.70	1.13
1.980	0.081	0.074	0.012	0.025	2.128	0.085	0.79	1.13

Table 11. Physical Properties of Cold Spray Aluminum.

Dimensions (cm)			Volume	Mass	Density	Uncertainty	Normalized	Mold
Length	Width	Thickness	(cc)	(g)	(g/cc)	(g/cc)	Density	Aspect Ratio
2.456	0.554	0.066	0.086	0.222	2.587	0.013	0.96	0.16
2.455	0.554	0.064	0.082	0.212	2.580	0.013	0.96	0.16
2.451	0.554	0.069	0.089	0.231	2.589	0.012	0.96	0.16
2.454	0.554	0.064	0.082	0.222	2.693	0.013	1.00	0.16
2.446	0.554	0.048	0.062	0.161	2.589	0.017	0.96	0.16
2.451	0.551	0.055	0.070	0.177	2.519	0.015	0.93	0.16
2.096	0.198	0.071	0.029	0.070	2.420	0.035	0.90	0.45
2.096	0.198	0.054	0.022	0.055	2.522	0.046	0.93	0.45
2.093	0.198	0.066	0.027	0.070	2.602	0.037	0.96	0.45
2.092	0.198	0.066	0.027	0.070	2.624	0.038	0.97	0.45
2.097	0.198	0.066	0.027	0.065	2.424	0.037	0.90	0.45
2.098	0.198	0.050	0.020	0.054	2.643	0.049	0.98	0.45
2.014	0.114	0.067	0.015	0.040	2.645	0.066	0.98	0.76
2.012	0.113	0.071	0.016	0.041	2.566	0.063	0.95	0.76
2.014	0.112	0.066	0.015	0.037	2.514	0.068	0.93	0.76
2.011	0.112	0.067	0.015	0.040	2.700	0.068	1.00	0.76
2.017	0.112	0.051	0.011	0.028	2.457	0.088	0.91	0.76
2.014	0.112	0.055	0.012	0.030	2.442	0.081	0.90	0.76
1.979	0.080	0.064	0.010	0.023	2.298	0.100	0.85	1.13
1.976	0.079	0.066	0.010	0.024	2.355	0.098	0.87	1.13
1.980	0.079	0.067	0.010	0.025	2.403	0.096	0.89	1.13
1.980	0.078	0.053	0.008	0.019	2.319	0.122	0.86	1.13

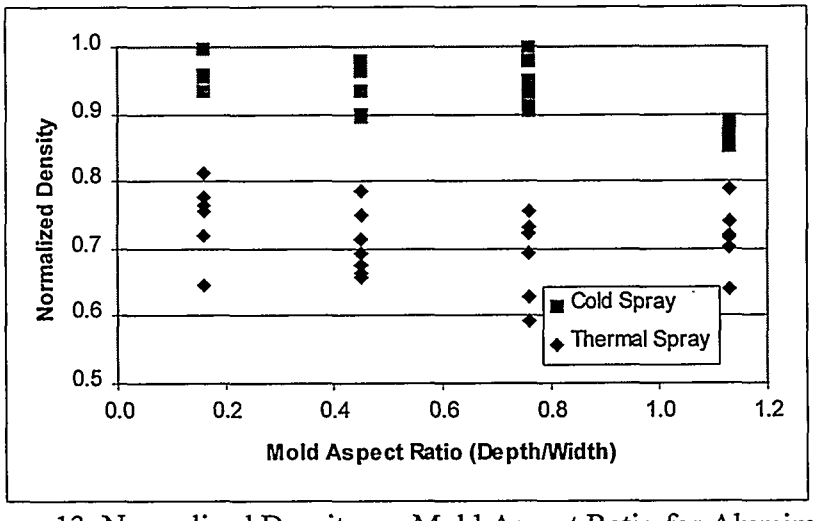

Figure 13. Normalized Density vs. Mold Aspect Ratio for Aluminum.

6.3.2 *Tensile*

Figure 14 shows the single specimen that was tested. Table 12 shows the modulus of elasticity and fracture stress for Thermal Spray aluminum, compared with aluminum alloy 1350 for reference [7]. The 1350 series alloy was chosen based on its material composition, 99.5% pure aluminum, which matches the material composition of the sprayed aluminum. Coatings typically have a lower modulus in tension because of the microcracking at the splat boundaries. Note: Because the 2% offset yield strength is unavailable for the aluminum tensile specimen, the fracture strength of the tensile specimen is compared to the tension strength of the 1350 alloy.

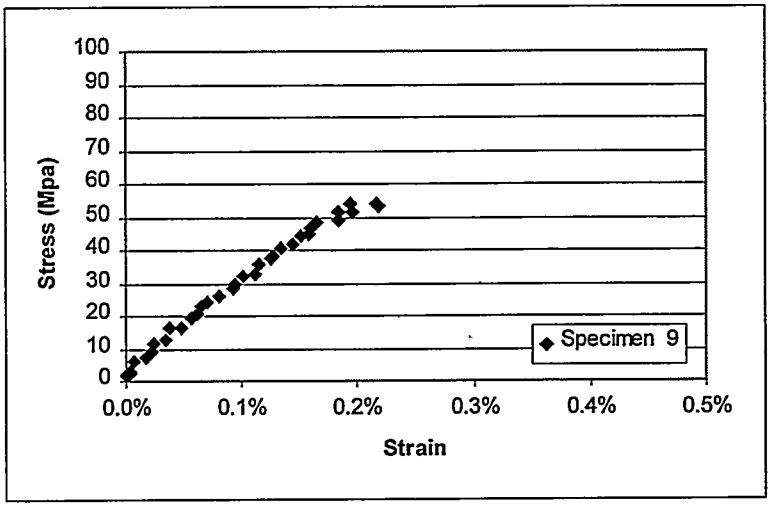

Figure 14. Engineering Stress vs. Engineering Strain for Twin-Wire Arc Thermal Spray Aluminum.

Table 12. Modulus and Yield Strength for Twin-Wire Arc Thermal Spray Aluminum.

	Modulus (GPa)	Fracture Strength (MPa)
Specimen 9	26	54
1350 Aluminum, Annealed	68	30
1350 Aluminum, Half Hard (H14)	68	95
1350 Aluminum, Hard (H19)	68	165

Figure 15 shows three Cold Spray test specimens. Table 13 shows the "pseudo" modulus of elasticity and ultimate tensile stress for Thermal Spray aluminum, compared with aluminum alloy 1060 for reference [7]. The 1060 series aluminum was chosen based on its material composition, 99.6% pure aluminum, which matches closely to the material composition of the Cold Spray Aluminum. Coatings typically have a lower modulus in tension because of the microcracking at the splat boundaries. Note: Because the 2% offset yield strength is unavailable for the aluminum tensile specimens, the fracture strength of the tensile specimens is compared to the tension strength of the 1060 alloy.

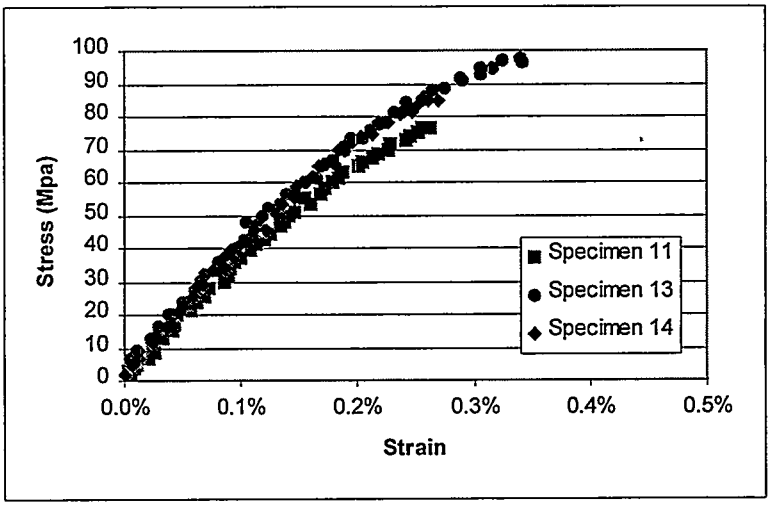

Figure 15. Engineering Stress vs. Engineering Strain for Cold Spray Aluminum.

Table 13. Modulus and Yield Strength for Cold Spray Aluminum.

	Modulus (GPa)	Fracture Strength (MPa)
Specimen 11	32	76
Specimen 13	36	98
Specimen 14	36	85
1060 Aluminum, Annealed	68	30
1060 Aluminum, Half Hard (H14)	68	90
1060 Aluminum, Hard (H18)	68	125

Figure 16 shows the two Cold Spray test specimens. Table 14 shows the "pseudo" modulus of elasticity and ultimate tensile stress for the Cold Spray Aluminum that was annealed. To anneal the aluminum, it was heated in air to 280°C and held there for 30 minutes. Then the temperature was increased to 310°C for an additional 30 minutes. Finally, the aluminum was air cooled to room temperature. These specimens are compared with aluminum alloy 1060 [7].

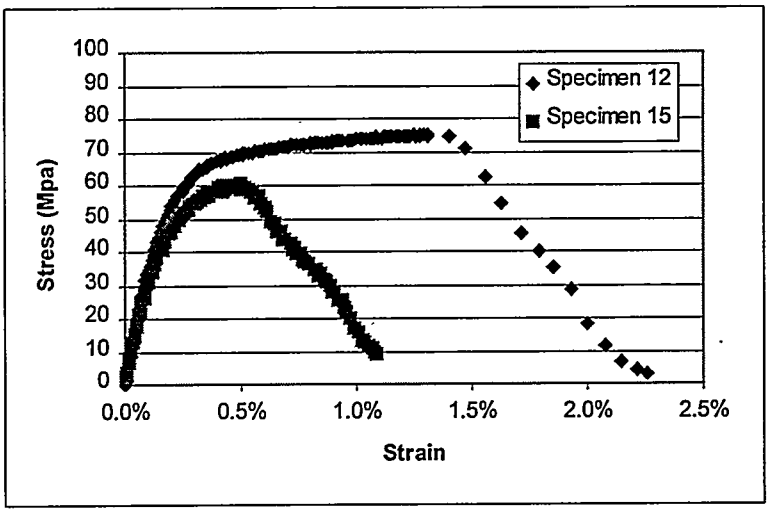

Figure 16. Engineering Stress vs. Engineering Strain for Cold Spray Aluminum, Annealed.

Table 14. Modulus and Ultimate Tensile Stress for Cold Spray Aluminum, Annealed.

	Modulus (GPa)	Yield Strength (MPa)
Specimen 12	29	68
Specimen 15	28	59
1060 Aluminum, Annealed	68	30
1060 Aluminum, Half Hard (H14)	68	90
1060 Aluminum, Hard (H18)	68	125

6.3.3 *Porosity*

Figure 17 displays the porosity vs. mold aspect ratio for Twin-Wire Arc Thermal Spray and Cold Spray Aluminum. Table 15 displays the average porosity, standard deviation, and percent accuracy for Twin-Wire Arc Thermal Spray Aluminum. Table 16 displays the average porosity, standard deviation, and percent accuracy for Cold Spray Aluminum.

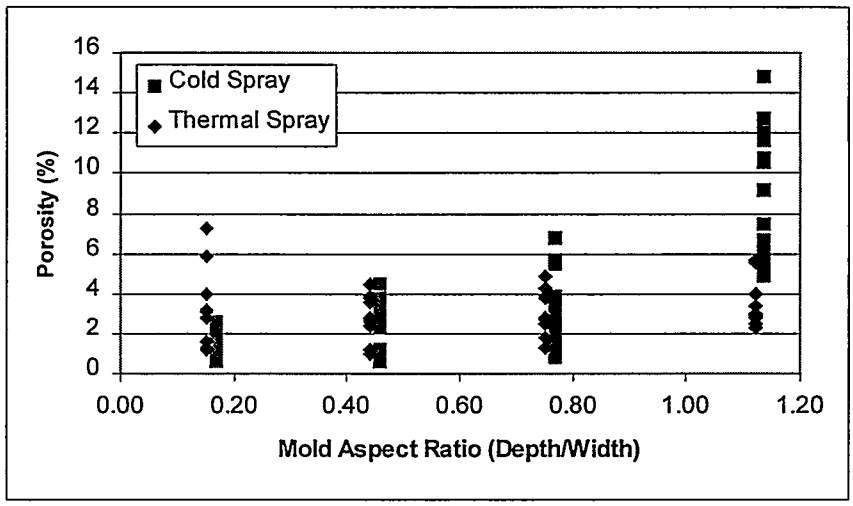

Figure 17. Porosity vs. Mold Aspect Ratio for Aluminum.

Table 15. Porosity Data for Twin-Wire Arc Thermal Spray Aluminum.

Mold Aspect Ratio	Number of Measurements	Average % Porosity	Standard Deviation	% Accuracy
0.16	10	3.13	2.07	41.71
0.45	10	2.84	1.12	25.07
0.76	10	3.05	1.13	23.43
1.13	10	3.46	1.23	22.42

Table 16. Porosity Data for Cold Spray Aluminum.

Mold Aspect Ratio	Number of Measurements	Average % Porosity	Standard Deviation	% Accuracy
0.16	20	1.53	0.61	17.73
0.45	20	1.98	1.19	26.93
0.76	20	2.66	1.71	28.76
1.13	20	9.37	4.02	19.21

6.3.4 Conclusions for Aluminum

An analysis of variance was used to test multiple data samples to determine whether the specimens were taken from the same population, and thus would be considered measurements of the same sample data. Figure 18 shows the results of this analysis for Twin-Wire Arc Thermal Spray and Cold Spray Aluminum.

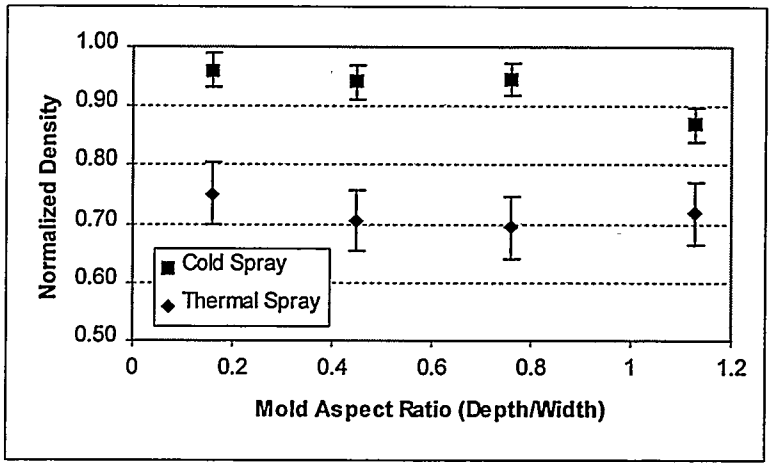

Figure 18. Mean Normalized Density vs. Mold Aspect Ratio for Aluminum.

Based on the analysis of variance for the density measurements, Twin-Wire Arc Thermal Spray Aluminum maintained a relatively uniform normalized density of 0.72, for all aspect ratios. The porosity of the specimens is likely to be lower than one minus the normalized density, because of the polishing of the specimens. When a specimen is polished, material can be deposited into pores, or metal smeared to close a small pore, causing a lower porosity reading. The porosity was approximately 3% for all aspect ratios.

Table 17 shows the correlation values between mold aspect ratio, average density, and average porosity for Twin-Wire Arc Thermal Spray Aluminum.

Table 17. Correlation Coefficients for Twin-Wire Arc Thermal Spray Aluminum.

Thermal Spray Aluminum	Correlation
Aspect Ratio and Density	-0.536
Aspect Ratio and Porosity	0.697
Density and Porosity	-0.170

The correlation coefficient for density and porosity does not meet the 0.9 criteria and therefore will not be used as an indicator to predict one variable from the other. The tensile specimen was brittle, making it difficult to obtain an accurate yield strength comparison, but a

"pseudo" modulus of elasticity was obtained and proved to be 38% of the 1350 alloy. Because the normalized density is lower than 0.9 and porosity is not a good predictor of density, Twin-Wire Arc Thermal Spray Aluminum is not a good candidate for further study.

Based on the analysis of variance for the density measurements, Cold Spray Aluminum maintained a uniform normalized density of 0.95 through an aspect ratio of 0.8 and then dropped off to 0.87 when the aspect ratio increased. Porosity increased from 2% to 9% when the aspect ratio exceeded 0.8. Table 18 shows the correlation values between mold aspect ratio, average density, and average porosity for Cold Spray Aluminum.

Table 18. Correlation Coefficients for Cold Spray Aluminum.

Cold Spray Aluminum	Correlation
Aspect Ratio and Density	-0.872
Aspect Ratio and Porosity	0.876
Density and Porosity	-0.987

The correlation coefficient relating density and porosity exceeded the 0.9 criteria, thus allowing the prediction of one variable from the other. The actual relationship between density and porosity is given by the following equation:

$$P = 88.3(0.97 - \rho)$$

where P is the percent porosity and ρ is the bulk density.

Ideally, the relationship would be given by the following relationship.

$$P = 100(1 - \rho)$$

The tensile specimens that were tested in the as-sprayed condition were brittle, making it difficult to obtain an accurate yield strength comparisons, but a "pseudo" modulus of elasticity was obtained and proved to be 51% of the 1060 alloy. Tensile specimens that were annealed showed greater ductility characteristics, allowing for an accurate yield strength comparison. The yield strength was more than twice that of the reference 1060 annealed aluminum alloy. Because the normalized density of Cold Spray Aluminum exceeded 0.9, there is a strong correlation between porosity and density, thus, which makes it a predictable material. Cold Spray Aluminum, consequently warrants further investigation. Additional studies of the minimum mold feature size that can be successfully filled by Cold Spray Aluminum is required.

There is one final observation to be made about the fill along the mold wall. A porous band was evident around the outer portions of the larger bulk specimens for each of the Twin-Wire Arc Thermal Spray materials. The Thermal Spray porous band is shown on the left side of Figure 19. The right side of Figure 19 is a photograph of a Cold Spray specimen. The Cold Spray material did not have a complete fill along one edge. This may be due to a preferred orientation of the jet stream coming from the Cold Spray nozzle that allows one side to fill to the edge of the mold and not to the other.

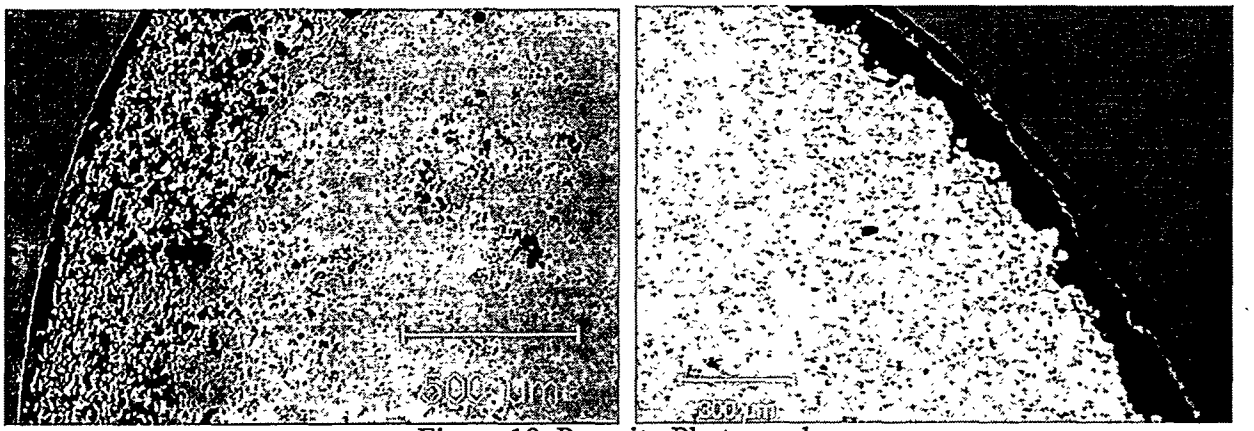

Figure 19. Porosity Photographs.
Left is a Twin-Wire Arc Thermal Spray specimen.
Right is a Cold Spray specimen.

7.0 Summary

Three specimen materials, UltraMachinable® Stainless Steel, BondArc®, and aluminum, were sprayed by using Twin-Wire Arc Thermal Spray. Based on the density and porosity data for these three specimen materials, Twin-Wire Arc Thermal Spray is not an adequate process for LIGA fabrication unless its deposition process can be improved. Only one material, aluminum, was sprayed using the Cold Spray process. Further investigation of the Cold Spray process is needed to study the minimum feature size that can be produced. Additionally, further investigation of additional Cold Spray materials would be worthwhile. Cold Spray of AISI 304 Stainless Steel, a second Cold Spray material, is planned for future testing in fiscal year 2000.

If subsequent testing determines that use of spray materials is a potential alternative to electroplating, future studies will determine whether spraying such materials could effectively produce quality mechanical parts that would be durable enough for practical LIGA designs.

8.0 References

1. M.F. Smith and R.A. Neiser, "Cold Spray Direct Fabrication-High Rate, Solid State Material Consolidation," Proc. Symposium V, Materials Research Soc., Fall '98 Mtg., Boston, MA, Nov. 30-Dec. 4, 1998.

2. H. El-Sobky, "Explosive Welding, Forming and Compaction," Edited by T.Z. Blazynski, Applied Science Publishers, London, 1983.

3. Metals Handbook Committee, "Metals Handbook," American Society for Metals, vol. 1, p. 984, Metals Park, Ohio, January 1975.

4. Hobart Tafa Technologies, Inc., Technical Data. Hobart/Tafa 88T UltraMachinable® Stainless Wire, 1992.

5. H.W. Coleman and W.G. Steele, "Experimentation and Uncertainty Analysis for Engineers," pp. 86–90. Wiley, New York, 1999.

6. D.T. Schamle, R.J. Bourcier, T.E. Buchheit, "Description of a Micro-Mechanical Testing System," SAND97-1608. Sandia National Laboratories, Albuquerque, NM, July 1997.

7. "Materials Engineering, Materials Selector 1990," Penton Publication, December 1989.

8. R.T. DeHoff and F.N. Rhines, "Quantitative Microscopy," McGraw-Hill, New York, 1968.

9. E.E. Underwood, "Quantitative Characterization of Microstructures," ASM International, 1993.

10. Hobart Tafa Technologies, Inc., Technical Data. Hobart/Tafa Arc Spray BondArc® Wire – 75B™, 1992.

11. T. R. Christenson, T. E. Buchheit, D. T. Schmale, and R. J. Bourcier, "Mechanical and Metallographic Characterization of LIGA Fabricated Nickel and 80% NI – 20% Fe Permalloy," SAND98-0906C. Sandia National Laboratories, Albuquerque, NM, April 1998.

12. Hobart Tafa Technologies, Inc., Technical Data. Hobart/Tafa Arc Spray Aluminum Wire – 01T, 1992.

9.0 Distribution

1	MS 0329	E.J. Garcia, 2614
1	MS 0329	F.J. Peter, 2614
1	MS 0329	D.W. Plummer, 2100
1	MS 0329	M.A. Polosky, 2614
1	MS 0333	T.E. Buchheit, 1835
6	MS 0367	M.F. Smith, 1833
1	MS 0367	M.F. Hosking, 1833
6	MS 0481	M.K. Decker, 2168
1	MS 0481	S.C. Holswade, 2168
1	MS 0481	K.D. Meeks, 2168
1	MS 0481	B.A Potts, 2168
1	MS 0603	T.R. Christenson, 1713
1	MS 1130	D.L. Gilmore, 1833
1	MS 1130	R.A. Neiser, Jr., 1833
1	MS 9018	Central Technical Files, 8940-2
2	MS 0899	Technical Library, 4916
1	MS 0612	Review & Approval Desk, 4912, For DOE/OSTI